

# Effects of Gas Pressure of Cold Spray on the Formation of Al-Based Intermetallic Compound

H. Lee, H. Shin, and K. Ko

(Submitted April 26, 2009; in revised form August 6, 2009)

In this paper, postannealing of cold-sprayed (CDGS) coatings for intermetallic compounds (IMC) in the matrix at low temperature and dependences of types and dispersion characteristics of intermetallic compounds on spraying pressure condition were investigated. The pressure prior to entering the gas heater was fixed at 0.7, 1.5, and 2.5 MPa. The relatively soft Al has been coated at low gas pressure condition (0.7 MPa) with severe plastic deformation owing to large peening effect. On the contrary, the Al particles coated at the higher pressure (1.5, 2.5 MPa) were not severely deformed. It was concluded that the pressure-controlled peening effects could alter the main route of Al consumption during annealing: eutectic or compounding of intermetallics. The thin and continuous IMC layer was formed at the interface with low pressure condition (0.7 MPa). On the other hand, the thick and discontinuous IMC layer was observed at the higher pressure condition (1.5, 2.5 MPa). Also, many eutectic pores were found in the Al-Ni composite coatings with lower gas pressure condition (0.7 MPa), but far less were found with high pressure environment.

**Keywords** Al, cold spray, gas pressure, intermetallic compound, postannealing

## 1. Introduction

Several intermetallic compounds have been studied extensively for possible structural applications, owing to their low density, high melting point, excellent thermal conductivity, and high level of resistance to corrosion and oxidation at elevated temperatures (Ref 1-5). Thick intermetallic compounds and IMC-embedded metal coatings are usually applied by thermal spray techniques, including plasma spray (Ref 1, 6), high-velocity oxy-fuel (Ref 7), wire-arc (Ref 8), and flame spray. However, these coating techniques are less suitable for use with aluminum containing raw materials, because the in situ melting or semi-melting process inside the spraying current can induce considerable oxidation of aluminum.

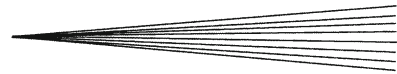
This article is an invited paper selected from presentations at the 2009 International Thermal Spray Conference and has been expanded from the original presentation. It is simultaneously published in *Expanding Thermal Spray Performance to New Markets and Applications: Proceedings of the 2009 International Thermal Spray Conference*, Las Vegas, Nevada, USA, May 4-7, 2009, Basil R. Marple, Margaret M. Hyland, Yuk-Chiu Lau, Chang-Jiu Li, Rogerio S. Lima, and Ghislain Montavon, Ed., ASM International, Materials Park, OH, 2009.

H. Lee, H. Shin, and K. Ko, Department of Materials Science and Engineering, Ajou University, Suwon 443-749, Korea. Contact e-mail: materialist@empal.com.

As an alternative, cold gas dynamic spray (CDGS; referred to simply as cold spray) has been suggested (Ref 9-15). And in the previous paper (Ref 16, 17), a nanocrystalline FeAl intermetallic compound, NiAl compound have been produced by cold spraying using mechanical alloyed powders and cold spraying of metal powder mixtures plus heat treatment could lead to the intermetallic compound formation (Ref 18-22). Instead of using precompound raw materials for intermetallic coating, the spraying of chemically pure powder and postannealing could be another option. Therefore, the controlling the compounding reaction at annealing stage is very important. Considering the most influential factor in reaction is solid-state diffusion, the defect generation mechanism during spraying has to be understood first. The processing parameters, such as gas pressure, gas temperature, and powder feeding rate, etc., could influence the particle velocity, and in turn, the coating properties such as coating density, defect density. In this work, the relationships between gas pressure and Al-based intermetallic compound formation were investigated.

## 2. Experimental Procedure

A custom-made cold spray system was used in this work. The particles were accelerated through a De Laval type of nozzle with a circular exit cross section (diameter, 7 mm; throat diameter, 1 mm; length of spray nozzle, 100 mm). Pure air, instead of the usual helium and nitrogen, was used as the main and the particle carrier gas. The pressure before entering the gas heater was fixed at 0.7, 1.5, and 2.5 MPa, and the temperature of the gas prior



to passing through the nozzle was 280 °C. The distance between the nozzle and the substrate was 10 mm. The particle sizes and shapes of the Al and Ni as purchased were confirmed by SEM (S-2400, Hitachi, Japan). Al on a pure Ni substrate, and Al-Ni composites were coated onto a pure Al substrate without sand-blasting the substrates with dimensions of 25 × 25 × 2 mm<sup>3</sup>. The powder composition ratio of Al and Ni was 75:25 wt.%, and the raw materials were dry blended with v-mill for 30 min. The coating thickness was about >500 μm. All the coated samples were annealed from 500 to 600 °C for 4 h in order to form the intermetallic compounds by solid state diffusion at the interface between the coating and the substrate. The heating and cooling rate is 5 °C/min. The microstructures and compositions of the coatings were measured by environmental scanning electron microscopy (ESEM) with energy dispersive spectroscopy (EDS) (Philips, XL 30 ESEM-FEG) and optical microscopy (OM).

### 3. Results and Discussion

#### 3.1 Pure Al coatings

The particle size of Al was under 77 μm with irregular shape and Ni particles were smaller than Al (3 μm) but aggregated (Fig. 1). Particle size distribution of Al powders was wide from 3 to 77 μm. Figure 2 shows the polished cross section images (OM) of as-coated Al coatings on Ni substrate coated with different pressures. In all cases, the coated Al powders have been plastically deformed and bonded to each other. After postannealing of as-coated Al specimens, the microstructure evolutions at coating interface were found to observe the intermetallic compound formation.

Figures 3 and 4 show OM images of Al coatings annealed at 550 and 600 °C, respectively. As shown in Fig. 3, the intermetallic compound formation of the annealed Al coatings on the Ni substrate had some unique features depending on applied pressures. While intermetallic compound layer was thin, but formed throughout the entire interface with low pressure (0.7 MPa), the thick and relatively discontinuous islands of intermetallic compound were observed with high pressure (1.5, 2.5 MPa). The higher the pressure is the more discontinuity [the percentage of the region without reaction between Al coating and Ni substrate at the interface (No IMC layer region)] increase. With increasing temperature of postannealing (Fig. 4), the growth of intermetallic layer proceeded in all samples to increase thickness. Thickening rate with the coating deposited at low pressure (0.7 MPa) was the smallest among all coatings, and other two cases were similar. But discontinuities in high pressure cases were sustained.

Figure 5 shows the additional results of thickness and continuity for IMC layers with different pressure and annealing time. Even the thickness of IMC layers was increased by extended annealing time, the IMC layer discontinuity of high pressure coatings increased further.

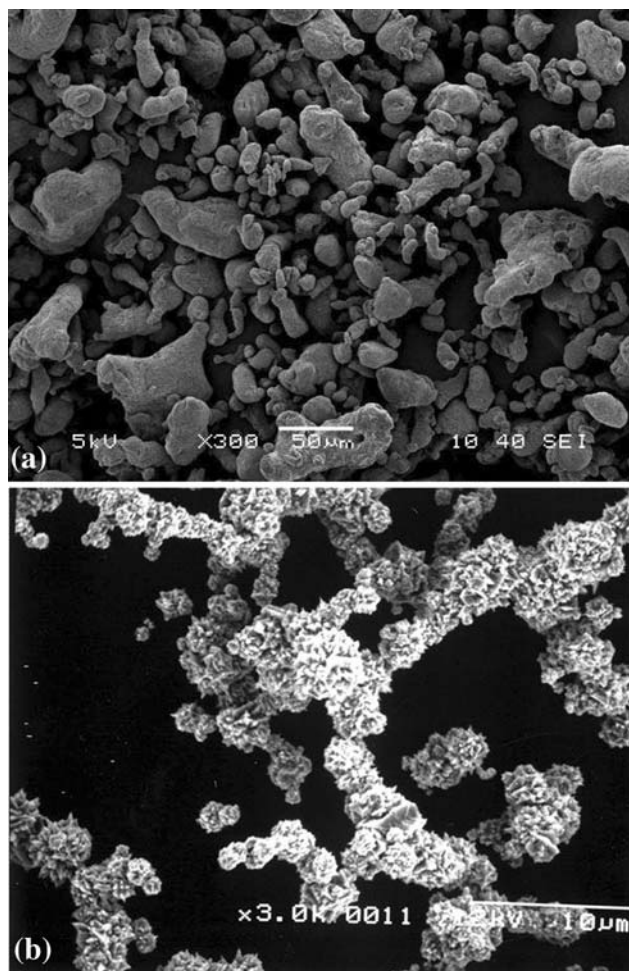
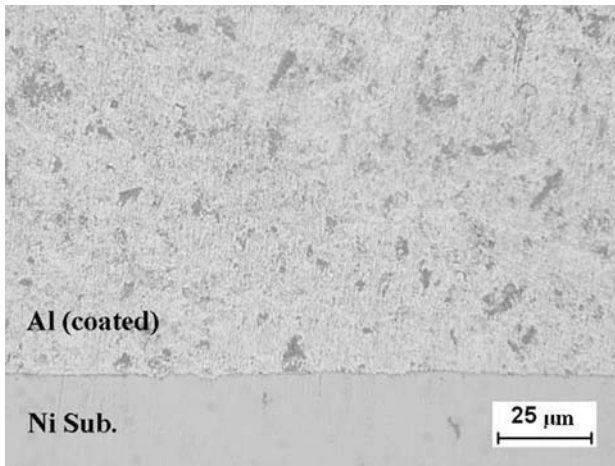


Fig. 1 SEM images of as-purchased powders used in the experiment. (a) Al (×300) and (b) Ni (×3.0k)

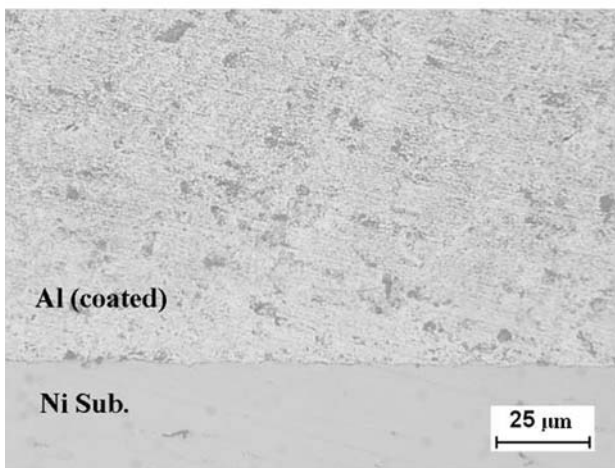
In addition, the evident contrast (light and dark at Al coating side and Ni substrate side, respectively) in intermetallic compound layers was observed clearly for annealed coatings with discontinuous morphology. In order to investigate the nature of contrast change, the composition of the interlayer was measured by EDS. Figure 6 shows EDS and backscattered images of Al coating annealed at 600 °C on Ni substrate. It was confirmed that the light contrast interlayer (in OM images, one on the Al coating side) was an Al<sub>3</sub>Ni intermetallic compound (Al rich) and the darker one (on the Ni substrate side) was Al<sub>3</sub>Ni<sub>2</sub> (Ni rich) (Ref 14).

#### 3.2 Al-Ni Mixture Coatings

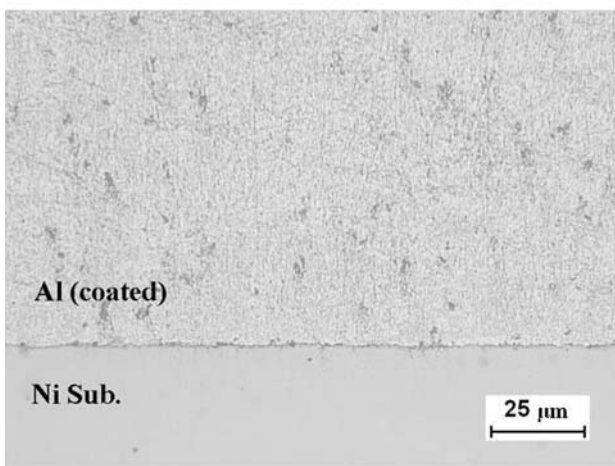
Figure 7 shows the polished cross section images (OM) of as-coated Al-Ni mixture coatings with different pressures. It was found that the matrix of coatings was Al regardless of the pressure condition and the Ni particles were well-dispersed and embedded in the Al matrix. Also, the Ni particles were sustaining aggregation size in the composite coatings. After annealing of as-coated Al-Ni



(a)

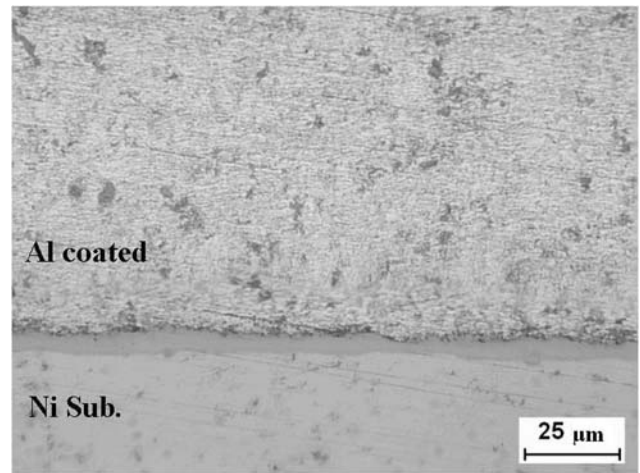


(b)

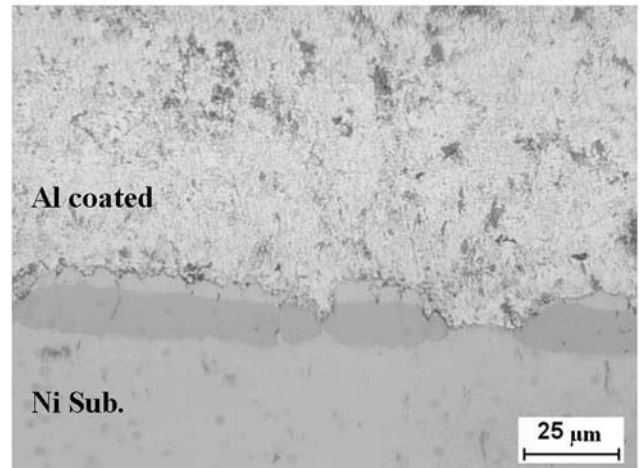


(c)

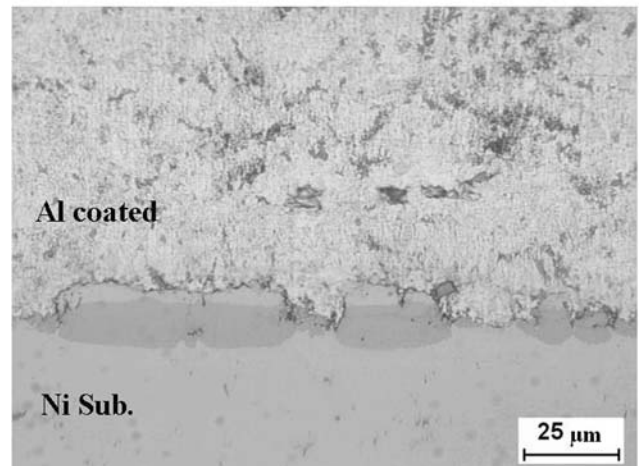
**Fig. 2** Polished cross section images (OM) of as-coated Al coatings with different pressure ( $\times 500$ ). (a) 0.7 MPa, (b) 1.5 MPa, and (c) 2.5 MPa



(a)

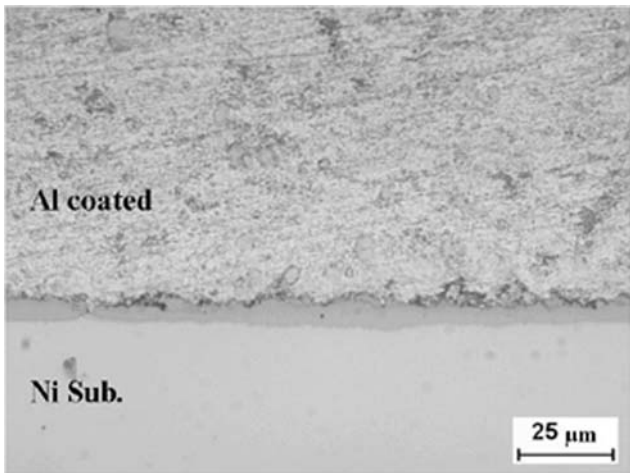


(b)

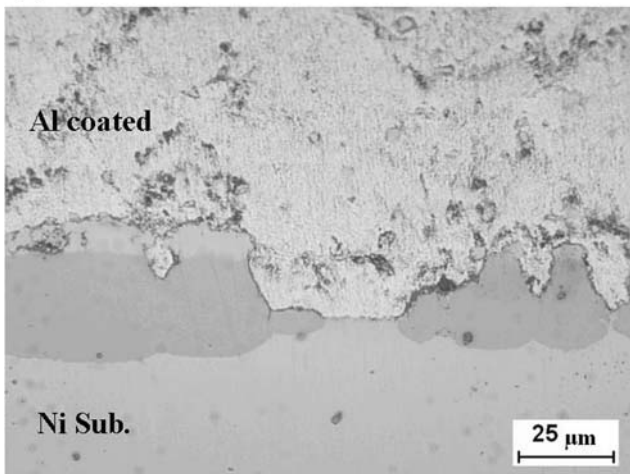


(c)

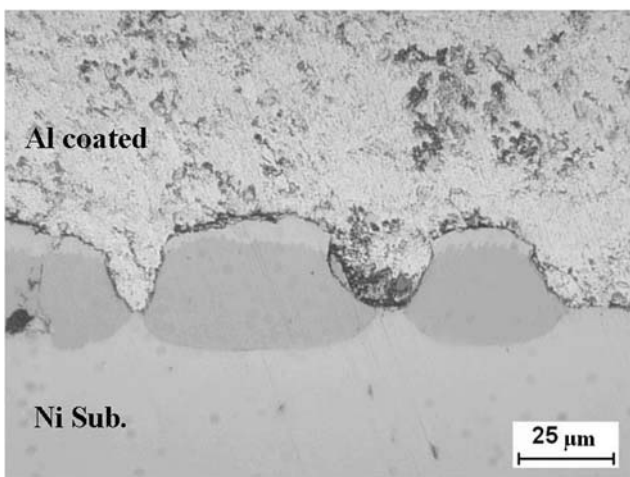
**Fig. 3** Polished cross section images (OM) of Al coatings annealed at 550 °C with different pressure ( $\times 500$ ). (a) 0.7 MPa, (b) 1.5 MPa, and (c) 2.5 MPa



(a)



(b)



(c)

**Fig. 4** Polished cross section images (OM) of Al coatings annealed at 600 °C with different pressure ( $\times 500$ ). (a) 0.7 MPa, (b) 1.5 MPa, and (c) 2.5 MPa

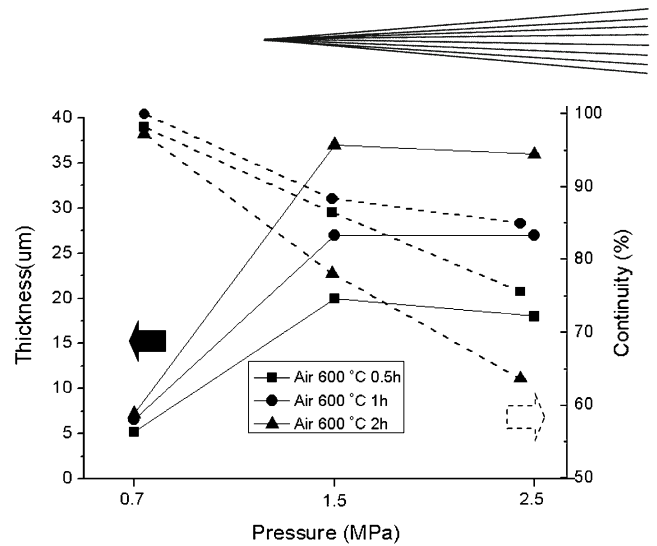


**Fig. 5** The thickness and continuity of IMC layer with different pressure

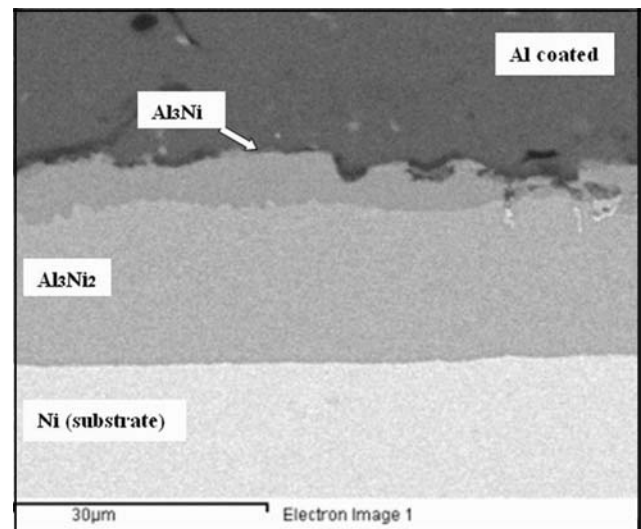
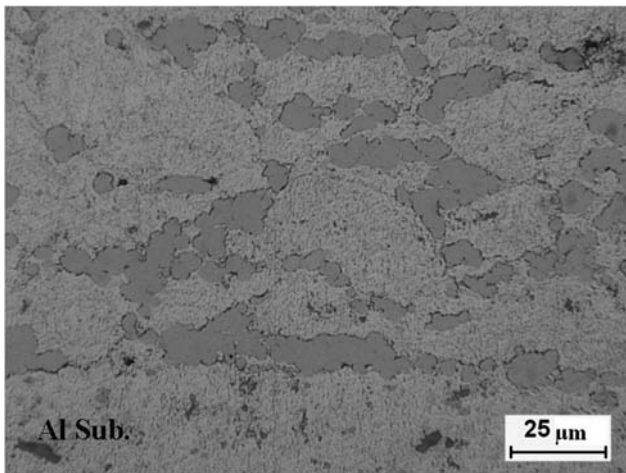


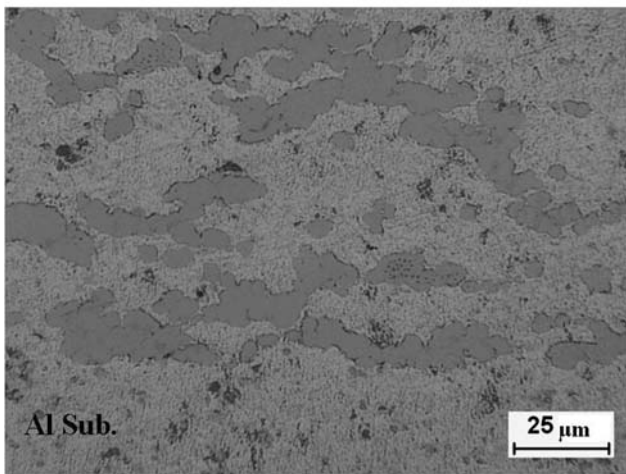
**Fig. 6** The backscattered electron images of annealed (600 °C) Al coating (1.5 MPa) using FESEM with EDS

composite coatings, as in previous pure Al/Ni-layered coating case, intermetallic compounds were found around Ni particles in all samples.

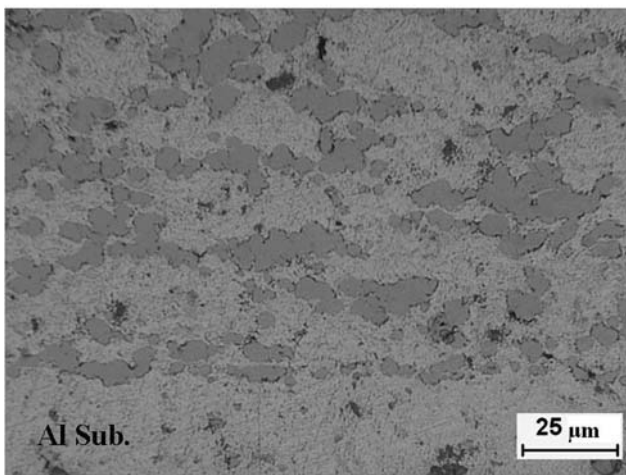
Figure 8 shows the backscattered electron images of annealed (600 °C) Al-Ni composite coating using FESEM with EDS. It was confirmed that the phases were  $Al_3Ni$  and  $Al_3Ni_2$  intermetallic compounds, respectively (Ref 13). However, the microstructure of annealed coatings looked differently depending on gas pressures. The many pores were observed in the composite coating with low pressure (0.7 MPa) due to the eutectic reaction between Al and Ni (Fig. 9a). On the other hand, the pores by eutectic reaction were not severe in size and number for high pressure



(a)



(b)



(c)

**Fig. 7** Polished cross section images (OM) of as-coated Al-Ni composite coatings with different pressure ( $\times 500$ ). (a) 0.7 MPa, (b) 1.5 MPa, and (c) 2.5 MPa

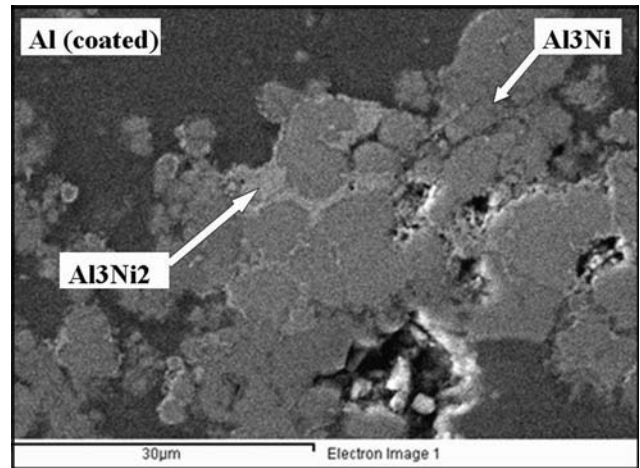
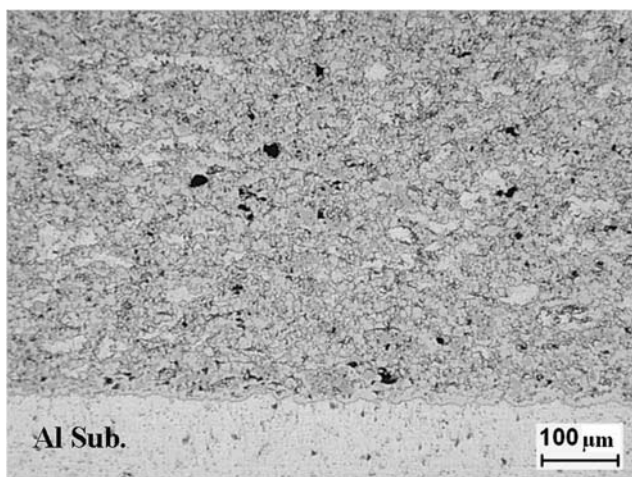
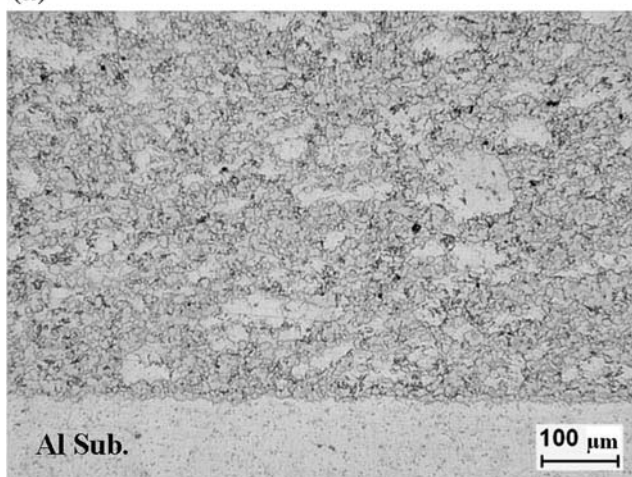


**Fig. 8** The backscattered electron images of annealed (600 °C) Al-Ni composite coating using FESEM with EDS

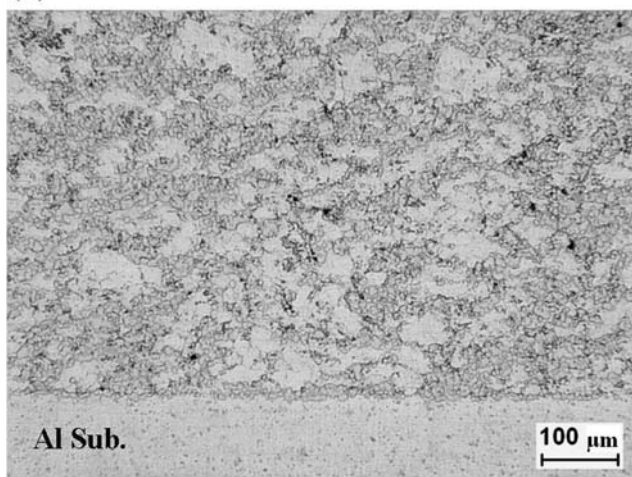
samples (1.5, 2.5 MPa) (Fig. 9b and c). With increasing the annealing temperature, the formation of eutectic pores became more aggressive owing to faster reaction rate in the low pressure coatings (Fig. 10a and 11a). However, in the case of the high pressure composite coatings, it seems that pore formation reactions had no significant differences even when the temperature of annealing increased (Fig. 10b, c and 11b, c). According to many researchers (Ref 23-27), in ultrasonically welded metal sheets, very high strain rate deformations can induce extremely high values of solid-state diffusivities. It was assumed that this enhanced diffusivity is induced by rapidly increased non-equilibrium vacancy concentration. By same token, it was assumed that the peening process, additional impounding action of re-bounced particles during cold spraying, could also create very high plastic strains resulting in extremely large excess vacancies on particles and/or particle interfaces. As reported in the previous research (Ref 15), the SEM images of fractured cross section Al coatings at different pressure were shown. The severe deformation and ductile fracture of particles in the Al coating was observed at low gas pressure condition by large peening of bounced-off Al particles. However, the accelerated Al particles by high pressure were not severely deformed when the particles were impacted onto substrate. In addition, this situation can provide appreciable reactivity among particles even at thermodynamically low temperature. According to phase diagram, eutectic reaction occurs at about 640 °C. So, a large numbers of pore from eutectic melting and solidifying below 600 °C could be a proof of nonequilibrium state. Al was consumed by two routes of reactions during annealing: eutectic formation and compounding of intermetallics. As coating pressure increased, the ratio of attaching to re-bounced (thus available for peening) particles increased. Therefore, the diffusivity of Al could not be enhanced as much as in low



(a)



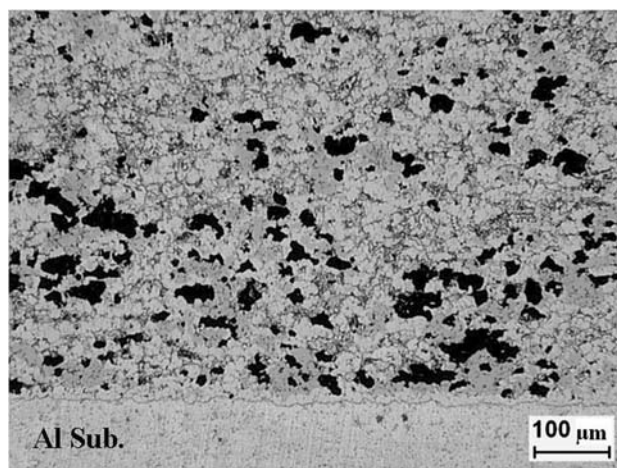
(b)



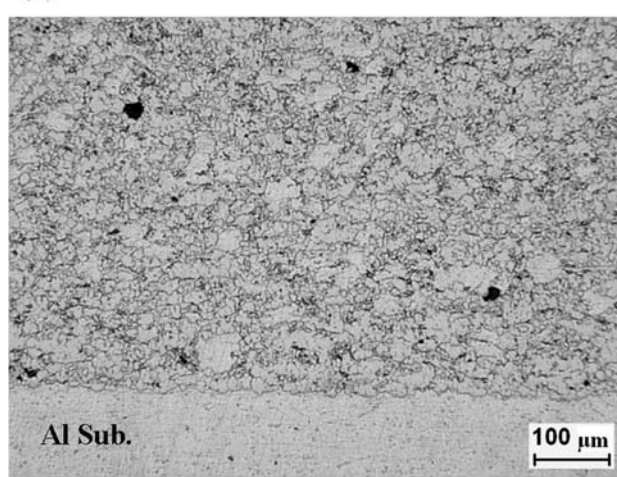
(c)

**Fig. 9** Polished cross section images (OM) of annealed (500 °C for 4 h) Al-Ni composite coatings with different pressure ( $\times 100$ ). (a) 0.7 MPa, (b) 1.5 MPa, and (c) 2.5 MPa

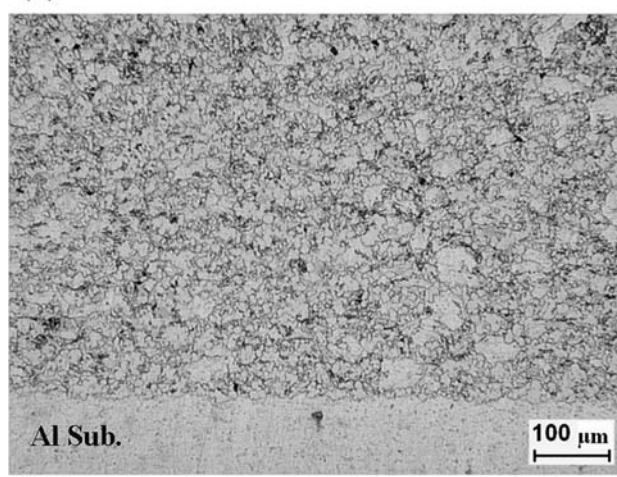
pressure case. Rather, it seems that the diffusivity of Al and hard Ni get closer and that intermetallic compounding route which needs more Ni than eutectic could devotes



(a)



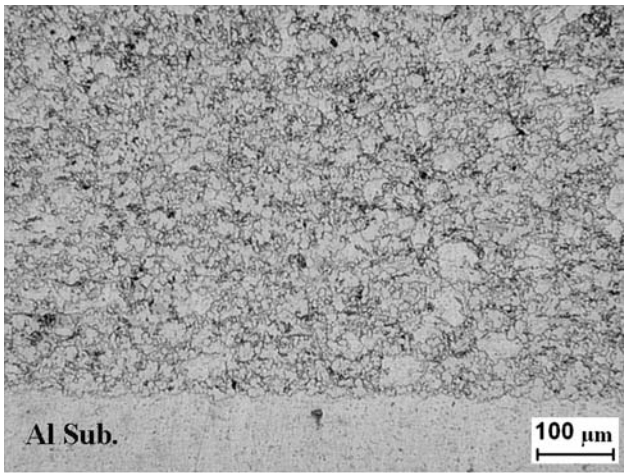
(b)



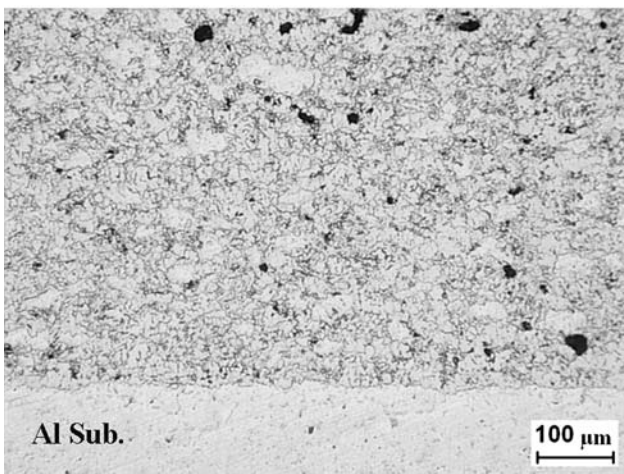
(c)

**Fig. 10** Polished cross section images (OM) of annealed (550 °C for 4 h) Al-Ni composite coatings with different pressure ( $\times 100$ ). (a) 0.7 MPa, (b) 1.5 MPa, and (c) 2.5 MPa

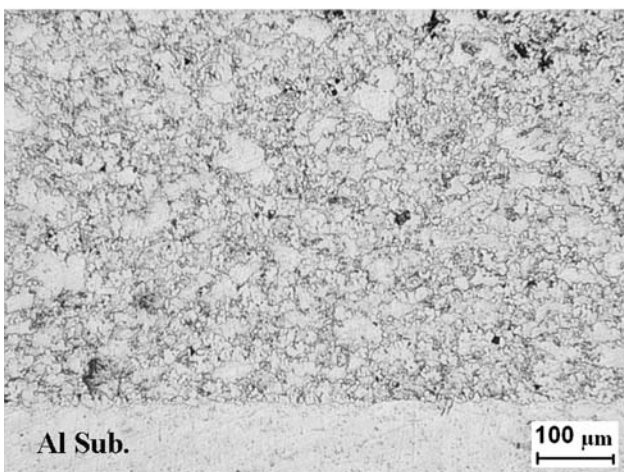
more to the consumption of Al particles. In this sense, pure Al/Ni experiments also can be analyzed. The good continuity of compound layer of low pressure coating



(a)



(b)



(c)

**Fig. 11** Polished cross section images (OM) of annealed (600 °C for 4 h) Al-Ni composite coatings with different pressure ( $\times 100$ ). (a) 0.7 MPa, (b) 1.5 MPa, and (c) 2.5 MPa

means large uniform nucleation at entire interface possibly due to high defect site creation at early stage of coating. Also, for the low thickening rate, it seems that large peening effects yields denser coating not so desirable for fast diffusion. On the contrary, relatively small amount of defects at the interfaces but loosely packed coating resulted in thick, discontinuous islands when pressure increased.

## 4. Conclusions

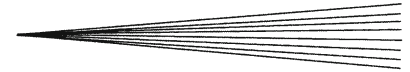
Effects of gas pressure on the morphology evolution of cold-sprayed Al-Ni system were investigated. Under low pressure, large amount of defects were created at interface. These effects gradually decreased as pressure increased. It was concluded that the peening effects which depend on gas pressure could alter the main route of Al consumption during annealing. Therefore, the controlling gas pressure condition used for spraying is very important with regard to the formation of intermetallic compounds in annealed cold-sprayed coatings.

## Acknowledgment

This research was supported by a grant from the Center for Advanced Materials Processing (CAMP) of the 21st Century Frontier R&D program funded by the Ministry of Knowledge Economy (MKE), Republic of Korea.

## References

1. K.A. Khor, Y. Murakoshp, M. Takahashi, and T. Sano, Plasma Spraying of Titanium Aluminide Coatings: Process Parameters and Microstructure, *J. Mater. Proc. Tech.*, 1995, **48**, p 413-419
2. C. Sierra and A.J. Vazquez, Dry Sliding Wear Behaviour of Nickel Aluminides Coatings Produced by Self-Propagating High-Temperature Synthesis, *Intermetallics*, 2006, **14**, p 848-852
3. L.I. Duarte, A.S. Ramos, M.F. Vieira, F. Viana, M.T. Vieira, and M. Kocak, Solid-State Diffusion Bonding of Gamma-TiAl Alloys Using Ti/Al Thin Films as Interlayers, *Intermetallics*, 2006, **14**, p 1151-1156
4. N.S. Stoloff, C.T. Liu, and S.C. Deevi, Emerging Applications of Intermetallics, *Intermetallics*, 2000, **8**, p 1313-1320
5. A.S. Ramos, M.T. Vieira, L.I. Duarte, M.F. Vieira, F. Viana, and R. Calinas, Nanometric Multilayers: A New Approach for Joining TiAl, *Intermetallics*, 2006, **14**, p 1157-1162
6. S.B. Mishra, K. Chandra, S. Prakash, and B. Venkataraman, Characterisation and Erosion Behaviour of a Plasma Sprayed Ni<sub>3</sub>Al Coating on a Fe-Based Superalloy, *Mater. Lett.*, 2005, **59**, p 3694-3698
7. J. Gang, O. Elkedimc, and T. Grosdidier, Deposition and Corrosion Resistance of HVOF Sprayed Nanocrystalline Iron Aluminide Coatings, *Surf. Coat. Tech.*, 2005, **190**, p 406-416
8. B. Xu, Z. Zhu, S. Ma, W. Zhang, and W. Liu, Sliding Wear Behavior of Fe-Al and Fe-Al/WC Coatings Prepared by High Velocity Arc Spraying, *Wear*, 2004, **257**, p 1089-1095
9. H. Lee, Y. Yu, Y. Lee, Y. Hong, and K. Ko, Cold Spray of SiC and Al<sub>2</sub>O<sub>3</sub> with Soft Metal Incorporation: A Technical Contribution, *J. Therm. Spray Technol.*, 2004, **13**(2), p 184-189



10. H. Lee, Y. Yu, Y. Lee, Y. Hong, and K. Ko, Thin Film Coatings of  $WO_3$  by Cold Gas Dynamic Spray: A Technical Note, *J. Therm. Spray Technol.*, 2005, **14**(2), p 183-186
11. H. Lee, Y. Yu, Y. Lee, Y. Hong, and K. Ko, Interfacial Studies Between Cold-Sprayed  $WO_3$ ,  $Y_2O_3$  Films and Si Substrate, *Appl. Surf. Sci.*, 2004, **227**, p 244-249
12. H. Lee, S. Jung, S. Lee, Y. Yu, and K. Ko, Correlation Between  $Al_2O_3$  Particles and Interface of Al- $Al_2O_3$  Coatings by Cold Spray, *Appl. Surf. Sci.*, 2005, **252**, p 1891-1898
13. H.Y. Lee, S.H. Jung, S.Y. Lee, and K.H. Ko, Alloying of Cold-Sprayed Al-Ni Composite Coatings by Post-annealing, *Appl. Surf. Sci.*, 2007, **253**, p 3496-3502
14. H. Lee, S. Lee, and K. Ko, Annealing Effects on the Intermetallic Compound Formation of Cold Sprayed Ni, Al Coatings, *J. Mater. Proc. Tech.*, 2009, **209**, p 937-943
15. H. Lee, H. Shin, S. Lee, and K. Ko, Effect of Gas Pressure on Al coatings by Cold Gas Dynamic Spray, *Mater. Lett.*, 2008, **62**, p 1579-1581
16. Q. Zhang, C.J. Li, X.R. Wang, Z.L. Ren, C.X. Li, and G.J. Yang, Formation of NiAl Intermetallic Compound by Cold Spraying of Ball-Milled Ni/Al Alloy Powder Through Post Annealing Treatment, *J. Therm. Spray Technol.*, 2008, **17**, p 715-720
17. H.T. Wang, C.J. Li, G.J. Yang, C.X. Li, Q. Zhang, and W.Y. Li, Microstructural Characterization of Cold-Sprayed Nanostructured FeAl Intermetallic Compound Coating and Its Ball-Milled Feedstock Powders, *J. Therm. Spray Technol.*, 2007, **16**, p 669-676
18. T.S. Price, P.H. Shipway, D.G. McCartney, E. Calla, and D. Zhang, A Method for Characterizing the Degree of Inter-Particle Bond Formation in Cold Sprayed Coatings, *J. Therm. Spray Technol.*, 2007, **16**, p 566-570
19. H.T. Wang, C.J. Li, G.J. Yang, and C.X. Li, Effect of Heat Treatment on the Microstructure and Property of Cold-Sprayed Nanostructured FeAl/ $Al_2O_3$  Intermetallic Composite Coating, *Vacuum*, 2008, **83**, p 146-152
20. H.T. Wang, C.J. Li, G.J. Yang, and C.X. Li, Cold Spraying of Fe/Al Powder Mixture: Coating Characteristics and Influence of Heat Treatment on the Phase Structure, *Appl. Surf. Sci.*, 2008, **255**, p 2538-2544
21. T. Novoselova, S. Celotto, R. Morgan, P. Fox, and W. O'Neill, Formation of TiAl Intermetallics by Heat Treatment of Cold-Sprayed Precursor Deposit, *J. Alloy Compd.*, 2007, **436**, p 69-77
22. T. Novoselova, P. Fox, R. Morgan, and W. O'Neill, Experimental Study of Titanium/Aluminium Deposits Produced by Cold Gas Dynamic Spray, *Surf. Coat. Technol.*, 2006, **200**, p 2775-2783
23. W. Gao, Z. Liu, and Z. Li, Nano- and Microcrystal Coatings and Their High-Temperature Applications, *Adv. Mater.*, 2001, **13**, p 1001-1004
24. Z. Liu, W. Gao, K. Dahm, and F. Wang, Oxidation Behaviour of Sputter-Deposited Ni-Cr-Al Micro-Crystalline Coatings, *Acta Metall. Mater.*, 1998, **46**, p 1691-1700
25. W. Gao, Z. Li, and Y. He, High Temperature Oxidation Resistant Coatings Produced by Electro-Spark Deposition, *Mater. Sci. Forum*, 2001, **369**(372), p 579-586
26. B. Bhushan and X.D. Li, Nanomechanical Characterisation of Solid Surfaces and Thin Films, *Int. Mater. Rev.*, 2003, **48**, p 125-164
27. C. Suryanarayana, Mechanical Alloying and Milling, *Prog. Mater. Sci.*, 2001, **46**, p 1-184